Calculating Differential Collision Cross Sections for Li_2-Ne Collisions

Christopher Roth, Wesleyan University Physics Department, QAC Apprenticeship 2013

Introduction

For the large majority of three-body systems, no exact solution exists. These systems are often analyzed with computational models. While quantum-mechanics provides the most accurate description of the physics of molecular systems, quantum models are still too computational demanding to be pragmatic in many cases. In such systems, classical models provide a very good approximation for collision dynamics.

In order to calculate collision cross sections classically for $Li_2 - Xe$ collisions, continuous vibrational and rotational actions must be assigned to discrete rovibrational states. Traditionally standard histogram binning has been used, in which the vibrational and rotational actions are rounded to the nearest whole numbers that represent a quantum state. However, expressing the cross section as a derivative with respect to the vibrational and rotational actions may improve the connection between classical and quantum mechanics (1). These cross sections are henceforth referred to as differential cross sections. Collision cross sections for $Li_2 - Xe$ collisions were calculated using both of these methods and compared.

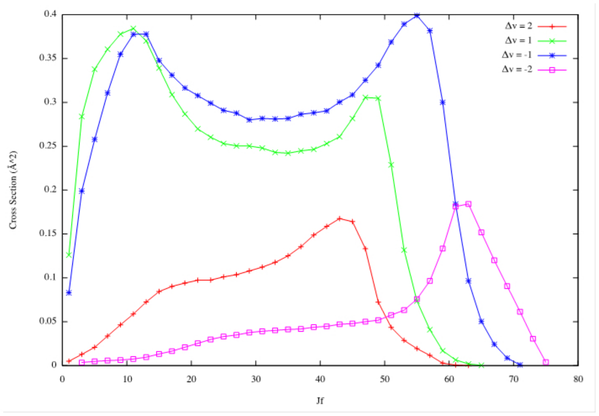

Figure 1: Collision cross sections at *2400 cm*$^{-1}$ for $v_i = 2, j_i = 3$ using standard histogram binning

Method

22 million trajectories were calculated using *a* $Li_2 - Xe$ potential (2), at an energy of *2400 cm*$^{-1}$ from an initial state $v_i = 2, j_i = 3$. The trajectories were assigned to final rovibrational states using standard histogram binning and Gaussian binning, in which the trajectories are weighted by Gaussians centered at the vibrational and rotational actions of quantum-mechanical states (3). Gaussian Binning was conducted for a range of standard deviations from *.01-.32*.

In order to calculate the differential cross sections, a generalized power law curve of the form $ax^b + c$ was fitted to the collision cross section as a function of Gaussian standard deviation. The contribution of individual points to the fit was weighted by error bars and the points were not used if their error bars exceeded *5%* of their value. The intercept of the curve was taken to be the differential cross section.

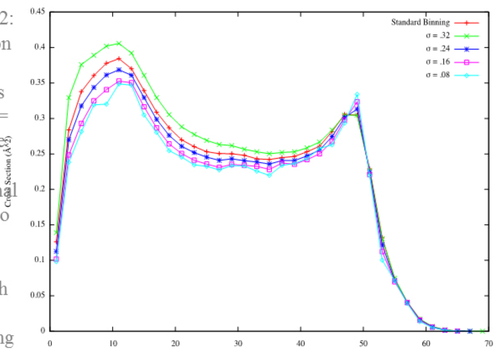

Figure 2: Collision cross sections for $\Delta v = +1$. The low rotational excitation peak (left) is diminished by shrinking the standard deviation while the high rotational excitation (right) is augmented. Similar effects are seen for the $\Delta v = -1$ distribution.

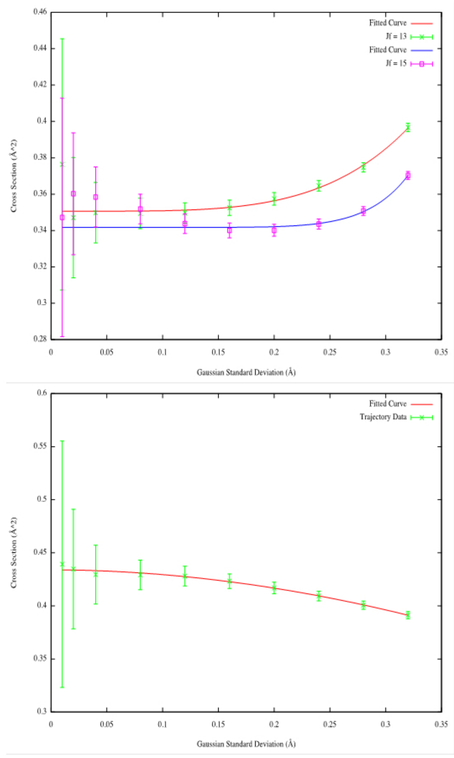

Figures 3a, 3b: Collision cross sections at the peaks of the $\Delta v = -1$ distribution as a function of standard deviation, and fitted power law curves to describe the behavior as the standard deviation approaches zero. a) $j_f = 13$ and $j_f = 15$. Both cross sections decrease and approach similar values as the standard deviation goes to zero. b) $j_f = 55$. The cross section increases as the standard deviation goes to zero.

Results

For the bimodal distributions $\Delta v = -1, +1$, shrinking the standard deviation of the Gaussian reduces the cross-section of the low rotational excitation peak and increases the cross-section of the high rotational excitation peak (fig. 2, 3). The effect on the low rotational excitation peak is more pronounced.

For the $\Delta v = -2, +2$ distributions there is only a high rotational excitation peak. As the bin width is reduced, the high rotation peak increases slightly but the cross section at all other areas decreases (fig. 4a).

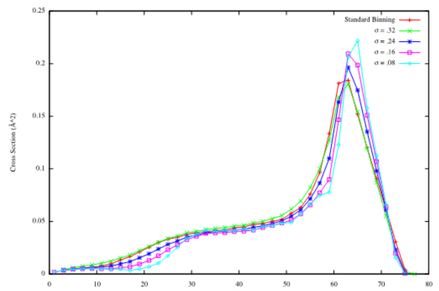

Figures 4a, b, c: Collision Cross Sections for $\Delta v = -2$. a) as a function of j_f. The peak is augmented for smaller standard deviations. b) as a function of standard deviation for $j_f = 63$ and 65. The peak shifts from $j_f = 63$ to $j_f = 65$. c) for $j_f = 17$. The cross section plummets to *10%* of its original value from shrinking the bin width.

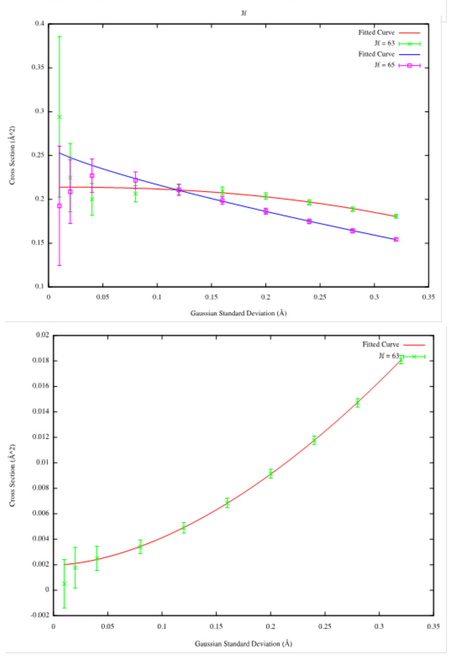

The $\Delta v = -2$ distribution is especially interesting. As the bin width is shrunk, the distribution experiences a peak shift from $j_f = 63$ to $j_f = 65$ (fig. 4b), and the cross section decreases by an order of magnitude in some areas (fig. 4c)

As a general rule of thumb, shrinking the bin width makes all of the vibrationally inelastic cross sections rotationally hot, meaning collisions with higher rotational excitation become more likely.

Table 1: Differential cross sections are calculated using curve fitting method discussed under Method. Note the order of magnitude difference between the differential cross section and the standard histogram cross section for $\Delta v = -2, j_f = 17$

ΔV	J_f	Standard Histogram Cross Section Å²	Differential Cross Section Å²	Percent Difference
2	43	.17	.18	10%
2	15	.084	.061	-27%
1	49	.30	.35	16%
1	11	.38	.35	-9.0%
-1	55	.40	.43	8.8%
-1	15	.35	.34	-1.7%
-1	13	.38	.35	-7.2%
-2	65	.15	.26	71%
-2	63	.18	.21	16%
-2	17	.017	.0020	-88%

Analysis

The trajectories for the vibrationally inelastic collisions may become more rotationally hot as the bin width is decreased because fewer collisions on the low vibrational excitation area of the bins are counted. For example as the bin around $\Delta v = 1$ is shrunk, fewer collisions with $\Delta v < 1$ will be counted. These collisions generally have less angular momentum transfer and may contribute to the low j_f cross-sections disproportionately. Although shrinking the bin also eliminates higher angular momentum collisions with $\Delta v > 1$, these collisions occur less frequently because of energetic and momentum transfer limits.

Generally, shrinking the bin width tended to decrease the average vibrationally inelastic cross sections across all final rotational quantum numbers. This is because the incidence of collisions decreases at an accelerating rate as $|\Delta v|$ increases. As the bin is shrunk, many more trajectories are lost on the low vibrational excitation end of the bin than the high vibrational excitation end, such that the density of trajectories over the bin decreases, thus decreasing the calculated cross-section.

This study could be greatly improved by increasing the number of trajectories. Data for low standard deviations is less precise because it samples fewer trajectories. Since these points have high leverage on the direction of the curves as standard deviation goes to zero, improvement of these points would improve accuracy.

Finally, a comparison to quantum mechanical calculations would be helpful to see which method of binning is closer to the true physics of the situation.

Acknowledgements

Thanks to professors Brian Stewart and Emmanuel Kaparakis for making this research possible, and Kirk Peterson for providing the potential function.

References

1) B. Stewart et al., *J. Phys. Chem.*, **104**, 10565(2000)

2) Kirk Peterson, private communication

3) J. Sierra et al., J. *Phys. Chem.*, **116**, 7413(2011)